

May 15, 2018

How universal are the density profiles of dark halos?

A. Huss¹, B. Jain^{1,2}, M. Steinmetz^{1,3}

adh@mpa-garching.mpg.de, bjain@pha.jhu.edu, msteinmetz@as.arizona.edu

ABSTRACT

We investigate the formation of virialized halos due to the gravitational collapse of collisionless matter using high-resolution N-body simulations. A variety of formation scenarios are studied, ranging from hierarchical clustering to monolithic radial collapse. The goal of these experiments was to study departures from the universal density profiles recently found to arise in cosmological settings. However, we found that even for models which exhibit quite a different formation history, the density and velocity dispersion profiles of the virialized halos are strikingly similar.

Power law density profiles do not result even in models with initial power law profiles and no initial substructure or non-radial motions. Such initial conditions give rise to a radial orbit instability which leads to curved velocity dispersion and density profiles. The shapes of the density profiles in all our models are well parameterized by the profiles of halos formed in a generic cosmological setting. Our results show that the universality of dark halo density profiles does not depend crucially on hierarchical merging as has been suggested recently in the literature. Rather it arises because apparently different collapse histories produces a near universal angular momentum distribution among the halo particles. We conclude that the density and velocity dispersion profiles of virialized halos in an expanding universe are robust outcomes of gravitational collapse, nearly independent of the initial conditions and the formation history.

Subject headings: cosmology: theory – cluster of galaxies – dark matter

1. Introduction

The hierarchical collapse of dark matter into virialized halos is likely to have played a key role in the formation of galaxies and clusters of galaxies. Several aspects of this process have been studied in recent years, in particular the role of initial conditions and of ongoing mergers in shaping the final structure of the dark matter halos. However, it remains an open question whether violent relaxation erases all information about the initial conditions and the formation history of halos. If it does not, then the density and velocity profiles of dark matter halos may bear imprints of the initial power spectrum as well as the cosmological density parameter Ω and the cosmological constant Λ .

Such a dependence between the initial power spectrum and the density profiles of virialized objects was pointed out by Hoffman & Shaham (1985) and Hoffman (1988). Their conclusions were based on the

¹Max-Planck-Institut für Astrophysik, Postfach 1523, 85740 Garching, Germany

²Department of Physics and Astronomy, Johns Hopkins University, Baltimore, MD 21218, USA

³Steward Observatory, University of Arizona, Tucson, AZ 85721, USA

secondary infall model of Gunn & Gott (1972), and the self-similar solution of Fillmore & Goldreich (1984) and Bertschinger (1985). These analytic calculations, however, were based on simplifying assumptions (e.g. spherical symmetry) and, therefore, could not consider all aspects of gravitational collapse. N-body simulations, which begin with generic initial conditions, provide an attractive alternative. Though the effects of gas dynamics are neglected, they are likely to represent a realistic description of the formation of galaxy clusters and the outer parts of galactic halos.

In recent years, multi-mass simulation techniques have been developed which allow one to investigate the formation of individual halos with high numerical resolution. Navarro, Frenk & White (1996, 1997) (hereafter NFW) have investigated the structure of dark matter halos which form in a cold dark matter (CDM) universe. They found that the density profiles of halos do not follow a power law, but tend to have a slope $\alpha = d \ln \varrho / d \ln r$ with $\alpha = -1$ near the halo center and $\alpha = -3$ at large radii. Over more the four orders of magnitude in mass, the density profiles follow a universal law, which can be parameterized by

$$\frac{\varrho(r)}{\varrho_b} = \frac{\delta_n}{\frac{r}{a_n} \left(1 + \frac{r}{a_n}\right)^2}. \quad (1)$$

The two parameters are the scale radius a_n which defines the scale where the profile shape changes from slope $\alpha > -2$ to $\alpha < -2$, and the characteristic overdensity δ_n . They are related because the mean overdensity enclosed within the virial radius r_{vir} is 180. Equation (1) differs slightly in its asymptotic behavior at large radii from the profile which was proposed by Hernquist (1990) to describe the mass profiles of elliptical galaxies. This profile, which goes like r^{-4} at large radii, was used by Dubinsky & Carlberg (1991) to fit the density distribution of halos which were formed in their CDM-like simulation.

Cole & Lacey (1996), Tormen, Bouchet & White (1996), Navarro, Frenk & White (1997), Huss, Jain & Steinmetz 1997 (hereafter HJS) and Moore et al. (1997), among others, have extended the original results of NFW to other initial spectra, to other cosmologies and to higher spatial and mass resolution. Most of the above studies show that halos which form in a variety of cosmological models are well described by equation (1). The scale radius and the central overdensity appear to be related to the formation time of the halo (Navarro et al. 1997). These results suggest that the density profile found by NFW is quite generic for any scenario in which structures form due to hierarchical clustering. The power spectrum and cosmological parameters only enter by determining the typical formation epoch of a halo of a given mass and thereby the dependence of the characteristic radius a on the total mass of the halo.

All these studies were based on initial particle distributions drawn from a Gaussian random field. Since cold dark matter scenarios have initial perturbations on all scales, the formation of halos generically proceeds by hierarchical merging of dark matter clumps. In this paper we instead use a set of artificial initial conditions, gradually increasing in complexity, to isolate the physical effects that determine the final properties of the halo. We control the degree of substructure by varying the velocity dispersion of the particles. The merging history of the halos varies between the two extremes of monolithic radial collapse and hierarchical merging.

2. Models and simulation parameters

The simulations used in this paper were performed using a N-body code which uses the special purpose hardware GRAPE (Sugimoto et al. 1989). The gravitational force is computed by direct summation over all particles with a Plummer force law. The Plummer softening parameter is $0.005h^{-1}$ Mpc in comoving units.

The initial overdensity $\Delta(x)$ inside a sphere of comoving radius x , is given by the power law

$$\Delta(x) = \Sigma (1 + z_i)^{-1} \left(\frac{x}{8 h^{-1} \text{Mpc}} \right)^{-1}. \quad (2)$$

The normalization Σ is set to 1.4, i.e. the halo formation time is the same as in the CDM model for which the power spectrum is normalized to $\sigma_8 = 0.6$. The size of the sphere at the initial redshift $z_i = 20$ is $15 h^{-1} \text{Mpc}$. The density field is set up by radially displacing particles from an initial glass-like particle distribution (White 1996). According to the Zel'dovich approximation (Zel'dovich 1970), the displacement vector is given by $\epsilon(x) = -x/3 \Delta(x)$. The initial particle velocities correspond to the growing mode of gravitational instability (in comoving units this is $u(x) = \dot{a}/a \epsilon(x)$). In addition varying amounts of initial velocity dispersion are added to the particle velocities. Details of the simulation technique used for the CDM model are described in an earlier paper (HJS).

The key parameters of the five models and the halos formed in each model are given in tables 1 and 2. All halos have in excess of 10^4 particles inside the virial radius at $z = 0$. The masses range from $0.3 - 0.5 \times 10^{15} h^{-1} M_\odot$ while the virial radii range from $1.1 - 1.4 h^{-1} \text{Mpc}$.

Of the five models listed in table 1, models I-IV use the power law initial profile of equation 2. Model I is constructed such that it is forced to undergo purely radial collapse. This is achieved by setting the tangential components of the gravitational force to zero, and by giving no initial dispersion in the particle velocities. Model II has the full three dimensional force but zero initial velocity dispersion. Models III and IV have increasing amounts of velocity dispersion given by σ_{3d} in table 1. These two models are designed to study to what extent the evolution of halos is affected by substructure which is produced by the initial velocity dispersion. Model V is the standard cold dark matter model. A detailed study of cluster formation in this model is presented in HJS.

3. Formation history and halo profiles

Figure 1 compares the formation of halos for the five considered models. Projected particle positions are shown in regions large enough to include nearly all particles. In the purely radial force model collapse proceeds inside out and a spherically symmetric halo forms in a smooth fashion. In model II which has no initial inhomogeneity or velocity dispersion a bar instability develops at redshifts less than 0.5. By $z = 0$ a distinct bar structure dominates the halo. This instability appears to be a radial orbit instability, found in collapse studies in a non-cosmological context (Polyachenko 1981; Merritt & Aguilar 1985; Carpintero & Muzzio 1995). We have confirmed the appearance of this bar instability under a variety of initial conditions. Our results thus demonstrate that the radial orbit instability can arise in a cosmological setting as well if

Table 1: Description of the five collapse models. All models assume $h = 0.5$; the CDM model is normalized to $\sigma_8 = 0.6$. σ_{3d} is the dispersion in the initial tangential (comoving) velocity in km/s.

Model	Description	Force	σ
I	spherical collapse	radial force	$\sigma_{3d} = 0$
II	spherical collapse	3d force	$\sigma_{3d} = 0$
III	spherical collapse	3d force	$\sigma_{3d} = 200$
IV	spherical collapse	3d force	$\sigma_{3d} = 2000$
CDM	Standard CDM		

the initial conditions are sufficiently smooth.

The range of models in figure 1 show increasing amounts of merging as the collapse proceeds. In models III and IV the clumpiness arises due to the initial velocity dispersion which leads to the aggregation of particles into small clumps at high redshift. These clumps in turn merge to form a single virialized halo at $z = 0$. The CDM model also shows hierarchical merging, though the collapse is more filamentary and occurs at higher redshift.

The density profiles of the models are shown in figure 2. We have plotted $r^2 \rho(r)/\rho_b$, where ρ_b is the background density, in order to show more clearly the curvature of the profile relative to an r^{-2} power law. Particles were binned such that each bin contains at least 100 particles. At high z , the density profile shows a radial infall pattern in all the models, with an r^{-2} profile developing in the inner regions. In model I, which has no non-radial forces, the r^{-2} profile remains stable and extends to the virial radius at $z = 0$. This slope is consistent with the predictions of the secondary infall model. However in the other three spherical models, by $z = 0.58$ the profile has developed significant curvature and is shallower than -2 in the inner regions and steeper near the virial radius. By $z = 0$ it is evident that with exception of model I all halos show a characteristic curved profile. The density profile of the CDM halo is well fit by the NFW profile. The profiles of the halos in models II-IV are very similar and are also adequately fit by the NFW form as shown in figure 2 (see figure 4 and discussion below for more details).

The velocity structure accompanying these density profiles at different redshifts is shown in figure 3. The radial streaming velocity, $v_r(r)$, indicated by the dashed-dotted line, clearly shows the infall pattern at high-redshift. At low redshift, $z \lesssim 1$, the halos become virialized and $v_r(r)$ is indeed consistent with zero. The velocity dispersions (radial and tangential shown by the solid and dotted lines, respectively) are small at $z \simeq 8$. For the lower redshifts, the radial dispersion approaches $\simeq 1000$ km/s. The tangential dispersion is nearly the same as the radial dispersion inside the scale radius, presumably due to the efficiency of violent relaxation in the inner regions, but is considerably smaller at larger radii. By construction, model I which is shown in the left-most panels, does not develop any tangential dispersion.

We have verified the features described above for other models not shown in figures 1-3. These include power law profiles for the initial overdensity with the logarithmic slope varying between -0.5 to -1.5 and a halo formed in a Hot Dark Matter model (see also HJS). In all cases, except for the initial conditions of model I, we recovered density profiles with characteristic curvature and velocity dispersion profiles similar to the ones shown in figure 3. Figure 4 shows the density profiles of four halos: three of them from power law initial profiles and the fourth from CDM initial conditions. It is evident that there is some scatter (typically $\simeq 20\%$) about the NFW-fit. We find that it is possible to fit the measured profiles somewhat better with a generalized profile, with the inner slope varying between -0.5 and -1 . This suggests that the NFW profile is not a unique best fit profile, at least for halos not formed in a hierarchical cosmology. It does however

Table 2: Parameters of the halos at $z = 0$. The mass within the virial radius M_{vir} is in units of $10^{15} h^{-1} M_\odot$, while r_{vir} and a_n are in h^{-1} Mpc.

Model	M_{vir}	r_{vir}	δ_n	a_n	c	$N(< r_{vir})$
I	0.30	1.13	-	-	-	10600
II	0.33	1.16	8300	0.22	5.4	11400
III	0.32	1.15	6400	0.24	4.7	11100
IV	0.29	1.12	11800	0.19	6.0	10200
CDM	0.50	1.36	13400	0.22	6.3	10800

provide an adequate fit given the scatter between the different halos. Only the halos of model I produced final density profiles that were well approximated by power laws in agreement with the analytic predictions of the secondary infall model (Fillmore & Goldreich 1984; Bertschinger 1985).

4. Discussion

We have simulated the collapse of dark matter halos with varying initial conditions. As shown in figure 1 the models are designed to vary the amount of sub-structure and merging in the collapsing halo. We found that even with a smooth initial particle distribution and minimal merging, the virialized density and velocity dispersion profiles of the halos are very similar to the halos formed in a cold dark matter cosmology. The density profile has logarithmic slope -2 at a characteristic radius and a slope shallower in the inner regions and steeper in the outer regions. It is well fit by the form proposed by NFW.

The only way we could get a power law density profile was to turn off the non-radial components of the gravitational force completely. Since this artificial condition can only be satisfied in a simulation, we conclude that dark matter halos resulting from gravitational collapse do not have power law profiles. Instead the density and velocity dispersion profiles have a nearly universal characteristic shape, independent of the initial conditions or the formation history.

Our results suggest that the key to universal density profiles does not lie in the hierarchical merging history of cold dark matter halos, as recently argued by Syer & White (1996). It is a more generic feature of gravitational collapse, which can be derived from the near universal behavior of the velocity field of the halo particles. The velocity dispersion profile grows with time in nearly the same way for halos in all the models. The mechanism by which angular momentum is acquired can vary, e.g. model II has little merging and instead shows a strong bar instability, but the resulting velocity dispersion profiles have similar shape.

NFW used hierarchical merging as embodied in the Press-Schechter scenario to model the variation of the scale radius a_n with halo mass and the cosmological model. To the extent that their results are empirically verified, they provide a useful guide to the variations of halo profiles. But our results suggest that the merging history is not a fundamental determinant of halo profiles, since the emergence of the characteristic scale radius occurs even in models with negligible merging. It would be interesting to pursue this issue further with detailed dynamical studies.

We wish to thank Julio Navarro, Dave Syer, Bepi Tormen, Scott Tremaine and Simon White for stimulating discussions. We are especially grateful to Bepi Tormen and Simon White for helpful comments on the manuscript. This work was partially supported by the Sonderforschungsbereich SFB 375-95 of the Deutsche Forschungsgemeinschaft.

REFERENCES

- Bertschinger E., 1985, *ApJS*, 58, 39
Carpintero D.C., Muzzio J.C., 1995, *ApJ*, 440, 5
Cole S., Lacey C., 1996, *MNRAS*, 281, 716
Dubinski J., Carlberg R. G., 1991, *ApJ*, 378, 496

- Fillmore J.A., Goldreich P., 1984, ApJ, 281, 1
- Gunn J.E., Gott, J.R., 1972, ApJ, 176, 1
- Hernquist L., 1990, ApJ, 356, 359
- Hoffman Y., Shaham J., 1985, ApJ, 297, 16
- Hoffman Y., 1988, ApJ, 328, 489
- Huss A., Jain B. & Steinmetz M., 1997, submitted to MNRAS (astro-ph/9703014)
- Merritt D., Aguilar L.A., 1985, MNRAS, 217, 787
- Moore B., Governato F., Quinn T., Stadel J., Lake G., 1997, submitted ApJ (astro-ph/9709051)
- Navarro J.F., Frenk C.S., White S.D.M., 1996, ApJ, 462, 563
- Navarro J.F., Frenk C.S., White S.D.M., 1997, ApJ, 490, 493
- Polyachenko V.L., Pis'ma Astr. Zh., 1981, 7, 142 (translated in Soviet Astr. Lett., 7, 79)
- Syer D., White S.D.M., 1998, MNRAS, 293, 337
- Sugimoto D., Chikada Y., Makino J., Ito T., Ebisuzaki T., Umemura M., 1990, Nat, 345, 33.
- Tormen G., Bouchet F.R., White, S.D.M., 1997, MNRAS, 286, 865
- White S.D.M., 1996, in Schaeffer R., Silk J., Spiro M., Zinn-Justin J., ed., Les Houches Session LX: Cosmology and Large-scale Structure, North-Holland, p. 349
- Zel'dovich, Y.B. 1970, A&A 5, 84

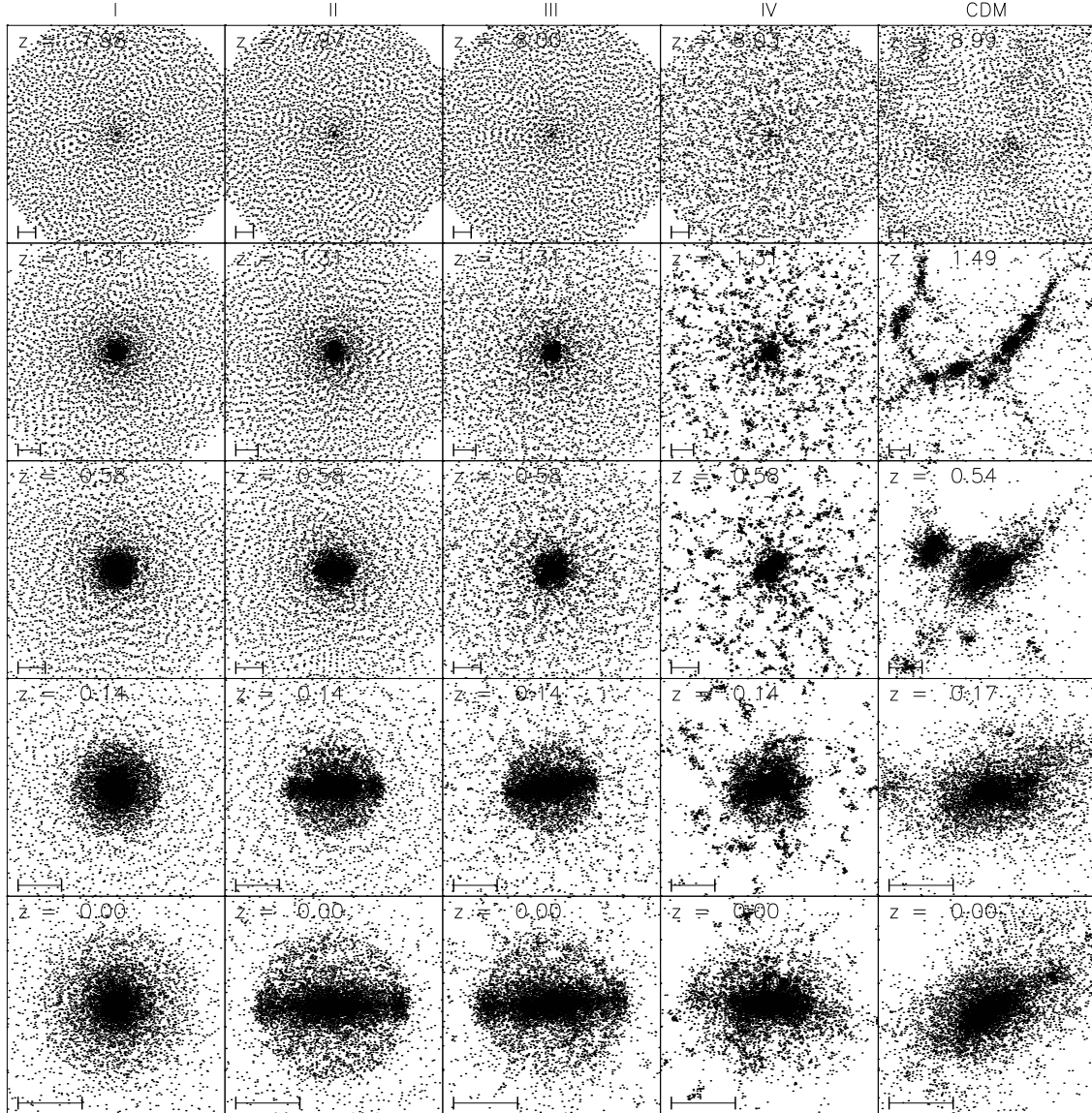


Fig. 1.— The projected particle distribution of halos at different redshifts is shown from top to bottom. The five models (see table 1) are shown from left to right. The side length in comoving units for the spherical collapse models I-IV is (from the top) 6.2 , 4.9 , 4.0 , 2.5 and $1.4 h^{-1}$ Mpc. For the CDM simulation the side length is 7.2 , 5.3 , 3.3 , 1.7 and $1.4 h^{-1}$ Mpc. A line of length $1 h^{-1}$ Mpc is shown within each box.

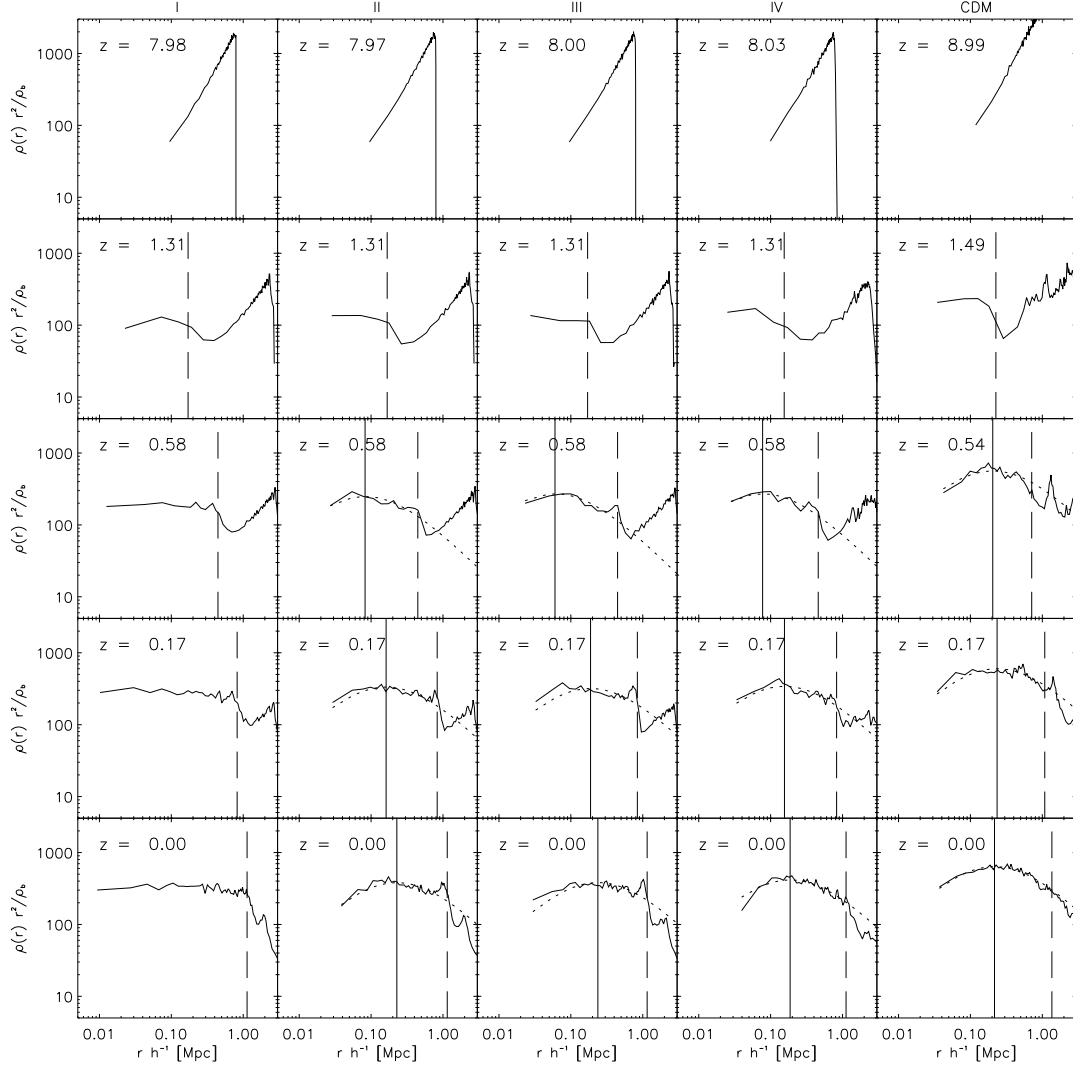


Fig. 2.— Density profiles shown at the same redshifts and for the same models as the particle distribution plot in figure 1. The vertical long dashed line is the virial radius r_{vir} , while the vertical solid line is the scale length a_n of the NFW profile. The dotted curves show the NFW-profile given in equation 1. It is evident that at low redshifts, $z \lesssim 1$, the density profiles of all the halos except model I are adequately fit by the NFW-profile.

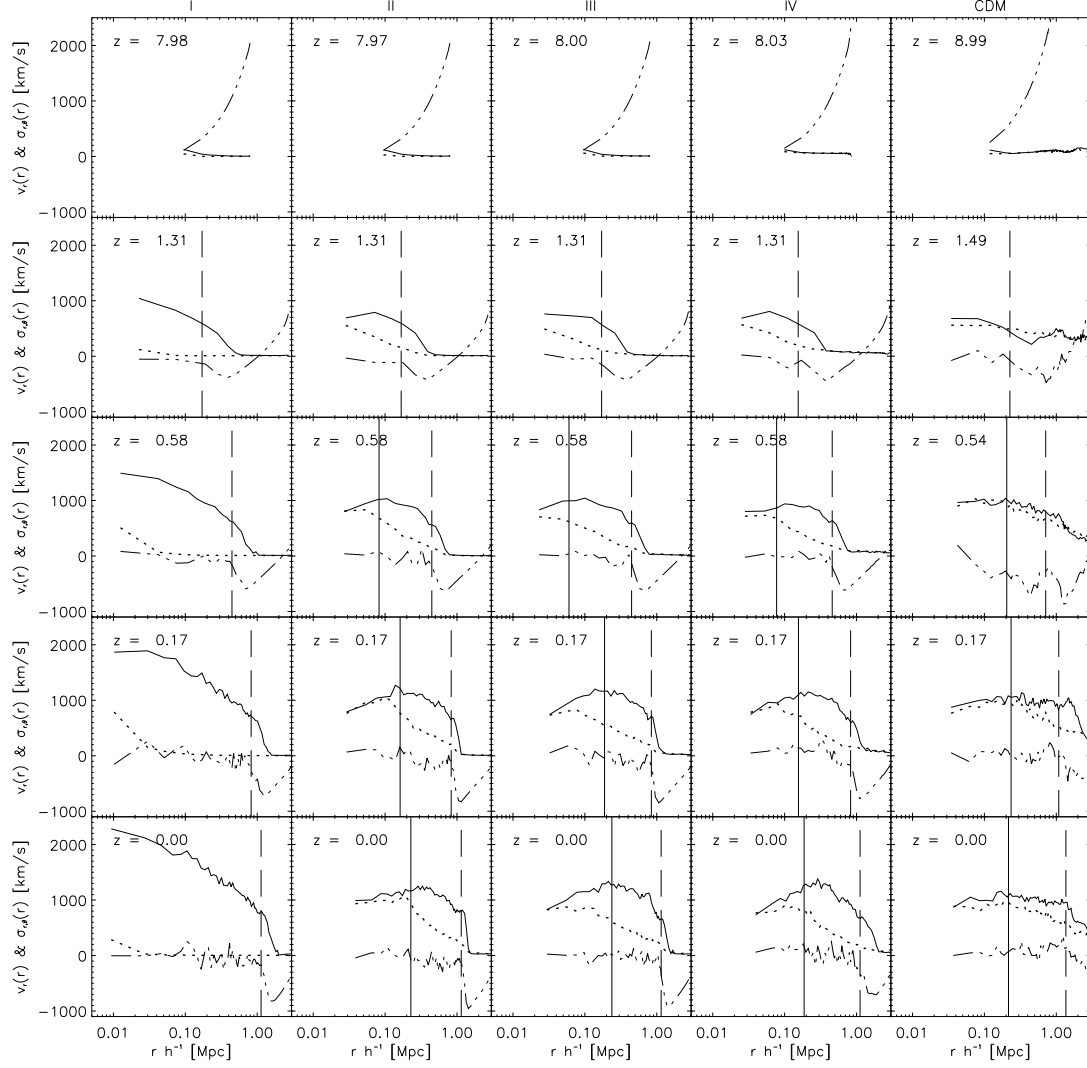


Fig. 3.— Radial streaming velocity $v_r(r)$ (dashed triple-dotted line) and the radial (solid line) and tangential (dotted line) velocity dispersions, $\sigma_r(r)$ and $\sigma_t(r)$ as a function of radius r . The models and redshifts are the same as in the previous two figures. The vertical long dashed line is the virial radius r_{vir} , while the vertical solid line is the scale length a_n of the NFW profile.

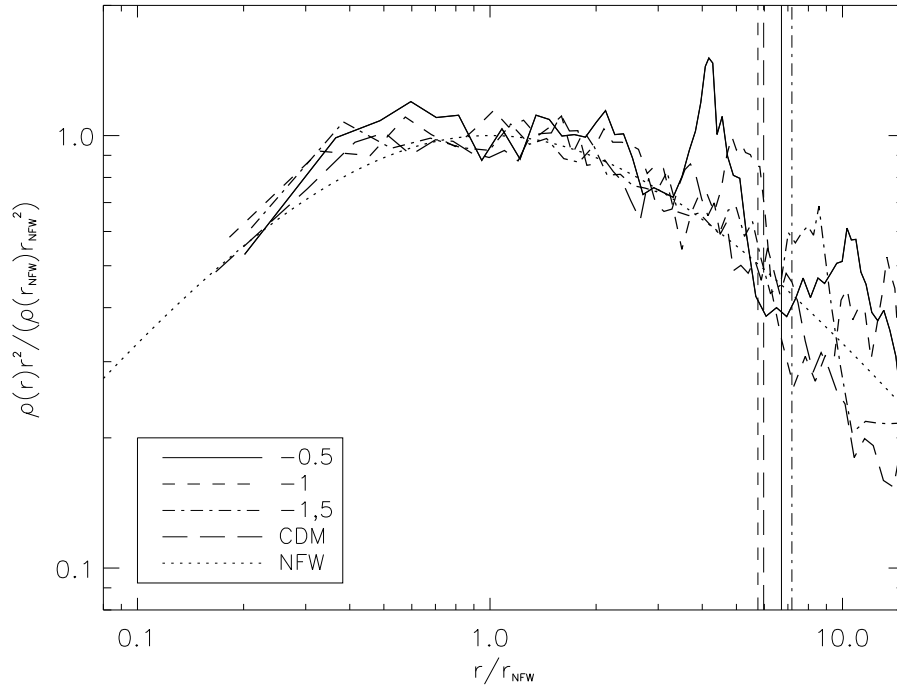


Fig. 4.— Density profiles at $z \simeq 0$ for three different power law models and the CDM model. The power law models plotted have initial profiles with logarithmic slopes = $-0.5, -1, -1.5$. The dotted curve shows the NFW fit, while the vertical dashed lines gives the virial radius for each halo.